Simulation of the Arthropod Central Complex: Moving Towards Bioinspired Robotic Navigation Control

Shanel C. Pickard[✉], Roger D. Quinn, and Nicholas S. Szczecinski

Case Western Reserve University, Cleveland, OH 44106, USA
sxp671@case.edu

Abstract. It is imperative that an animal have the ability to track its own motion within its immediate surroundings. It gives the necessary basis for decision making that leads to appropriate behavioral responses. It is our goal to implement insect-like body tracking capabilities into a robotic controller and have this serve as the first step toward adaptive robotic behavior. In an attempt to tackle the first step of body tracking without GPS or other external information, we have turned to arthropod neurophysiology as inspiration. The insect brain structure called the central complex (CX) is thought to be vital for sensory integration and body position tracking. The mechanisms behind sensory integration are immensely complex, but it was found to be done with an elegant neuronal architecture. Based on this architecture, we assembled a dynamical neural model of the functional core of the central complex, two structures called the protocerebral bridge and the ellipsoid body, in a simulation environment. Using non-spiking neuronal dynamics, our simulation was able to recreate *in vivo* behavior such as correlating body rotation direction and speed to activity bump dynamics within the ellipsoid body of the central complex. This model serves as the first step towards using idiothetic cues to track body position and orientation determination, which is critical for homing after exploring new environments and other navigational tasks.

Keywords: Sensory integration · Insect central complex · Control

1 Introduction

Navigating the world is a vital task for survival, and yet we take the ability to do so for granted. Insects and other arthropods, despite their small size, are capable of incorporating the endless stream of sensory information from their eyes, antennae, and other organs into real-time position and orientation updates in the brain, and use that information to decide where to go next (for reviews,

see [4, 7]). Understanding how the brain is able to seamlessly accomplish such a feat has been at the forefront of insect neurobiology [3, 11, 12]. The focus of these efforts has been to understand a brain structure known as the central complex (CX), which is thought to be vital for sensory integration and body position tracking.

As roboticists, we are tasked with giving our robots capabilities that we hope can one day be on par with our own. One of the basic necessities that our robots must have is the ability to accurately keep track of their body position relative to objects of interest in the environment. This is a challenge because the current approach to robotic control involves a thorough understanding of the task and environment on the part of the programmer, which must then be implemented as a well thought-out series of "if-then-else" statements. This becomes rather difficult when environments are not globally known, or are ever-changing (e.g. weather devastated locales, extraterrestrial landscapes). Thus, we build robot controllers using dynamical neural structures [10], which we believe will help us mimic animal brain structures and endow robots with animal-like navigation- and decision-making abilities.

1.1   Background: Tracking Body Position in the Arthropod CX

How the brain utilizes sensory information to determine body position at any given time and coordinate proper responses is not fully understood. Exciting results from the field of arthropod neurobiology have offered insight into brain substructures that appear to play a pivotal role in this task [3, 11]. The central complex is a brain structure found in all arthropods and is comprised, in many species, of four neuropils: the protocerebral bridge (PB), the fan shaped body (FB), the ellipsoid body (EB), and the noduli.

Wolff et al. contributed an excellent survey of central complex connectivity that showed a richly complex network between the PB, FB, and EB. Although this paper does not address functional roles of the cell types, it provides a detailed framework for the "wiring rules" of these neuropils [13]. More recently, physiological work elaborated on the connectivity between the PB and EB and found that these two structures have coordinated activity that correlates to rotational body movement [3, 11]. Specifically, a recursive excitatory connectivity between the eight column cells of the PB and the eight wedge cells of the EB maintain activity within these structures that correspond to body rotational location and speed. Three key tenants of CX behavior that our simulation captures in this paper include:

1. The direction of body rotation dictates direction of activity bump movement in the EB layer.
2. The body's rotational speed correlates to bump activity speed in the EB.
3. The activity in the PB leads activity in the EB.

1.2   Background: Mathematical Models of the Arthropod CX

Several recent models have sought to reproduce and explain the dynamics of the CX, and how it may give rise to navigational abilities. The work of Webb et al. created an "anatomically constrained" model of the CX, in which they mimicked the connectivity described in the previous subsection, and used the resulting model to control a robot's homing abilities after exploring an environment [8]. They found their model to be robust, with overall functionality not depending strongly on parameter values, as in our work. They constructed their model from static sigmoidal neurons, with recurrent connections added where necessary for memory dynamics. The work of Hirth et al. created a recurrent neural network simulation of the ellipsoid body, and showed that it was capable of aiding in decisions about which direction to go to navigate toward a goal based on its current orientation and simplified visual input [2]. This was accomplished by finding mappings between sensory information and the ellipsoid body that produce the intended goal-seeking behavior in a simulated agent. The result was that this agent could navigate a simple maze toward a goal. Both of these works have used their CX model in a closed-loop way to produce behavior in a simulated or hardware agent, something that we have not yet tested with our model. However, this paper presents a similarly biologically-constrained model, which uses dynamical neural components to reproduce key features of the CX, as listed in the previous subsection. Specifically, our CX model enables the use of idiothetic sensory input to track the body's heading.

2   Methods and Results

2.1   *In Silico* Model

We constructed a neural model in Animatlab, a 3D graphics environment for neuromechanical simulations [1], using the aforementioned recursive excitatory connectivity between the PB and EB (Fig. 1). This schematic represents the assembly of the processing layers of our simulation while remaining representative of *in vivo* neuronal connectivity. As seen in Fig. 1A, the P-ENs are the column cell projections that originate in the PB and synapse with EB wedge cells (also called E-PGs). Figure 1B shows the returning projections of the EB wedge cells to the PB, thereby completing the recursive loop. Internal to the EB, Fig. 1C shows an example of the inhibition circuit; when an EB wedge is active, the inhibition of connecting wedges is proportional to the activity magnitude.

   The neurons themselves were modeled with linear conductance dynamics [10] to represent time dependent electrical properties. The voltage across each neuron's cell membrane, U, has the dynamics

$$C_{\mathrm{mem}}\frac{dU}{dt} = I_{\mathrm{ion}} + I_{\mathrm{syn}} + I_{\mathrm{app}}. \tag{1}$$

   Equation 1 states that the current across the cell membrane (left hand side of the equation) is equivalent to the incoming, applied current I_{app}, plus the current
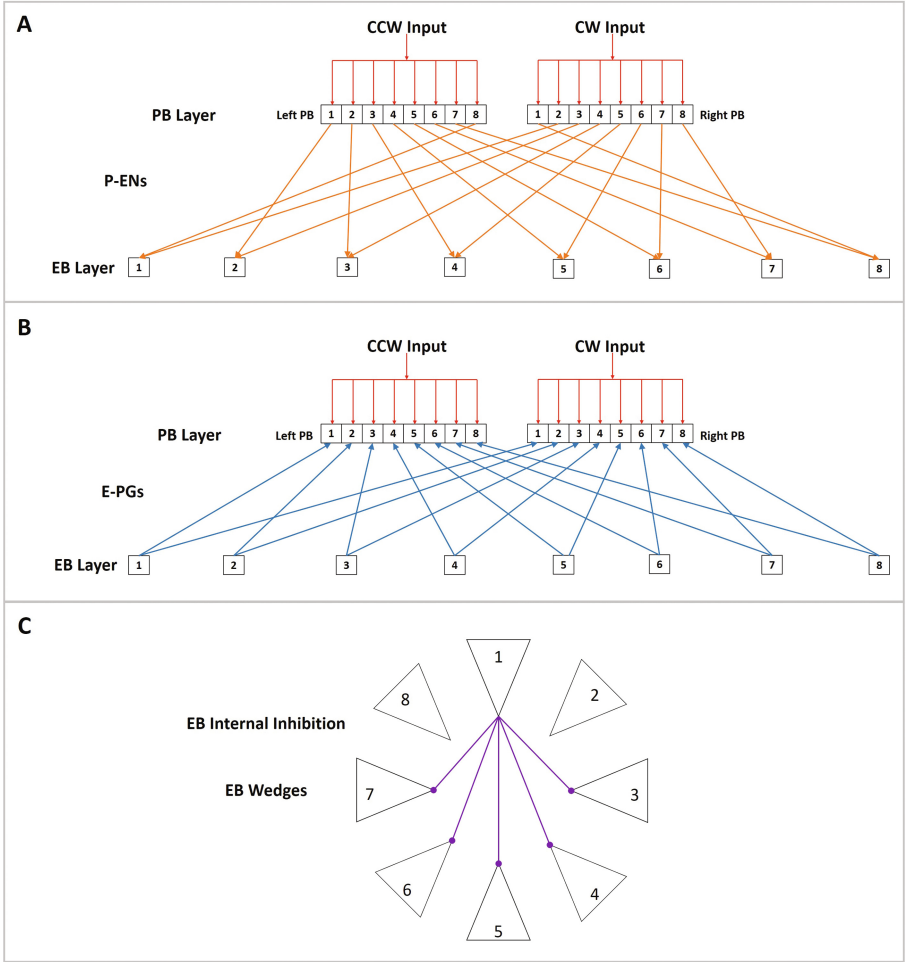
Fig. 1. Connectivity of the model. (A) The P-EN excitatory neurons project from PB to EB. Each P-EN connects in a counterclockwise fashion to the EB. (B) The E-PGs, project from the EB to the PB. (C) Internal EB inhibition example. Each wedge internally connects to the other wedges, except for the two immediately adjacent wedges. (Color figure online)

due to ion flux through membrane gates, I_{ion}, plus the current across the synapse (transmitter induced), I_{syn}. Plugging in for the currents, Eq. 1 becomes

$$C_{\text{mem}} \frac{dU}{dt} = g_{\text{mem}} \cdot (U_{\text{rest}} - U) + g_{\text{syn}}(t) \cdot (E_{\text{syn}} - U) + I_{\text{app}}, \tag{2}$$

where C_{mem} is the membrane capacitance, g_{mem} is the membrane conductance constant, U_{rest} is the equilibrium potential constant (voltage where inward and

outward currents are equal), $g(t)_{\mathrm{syn}}$ is the time variable conductance of the synapse, and E_{syn} is the reversal potential of the synapse.

These equations contain many parameter values that must be tuned. In the past, we have developed methods for selecting parameter values based on the function of network components [10]. Therefore, we were able to directly assemble a network whose overall behavior satisfied our goals in Subsect. 1.1. We believe this is sufficient for two reasons. First, related studies have found the function of the CX structure not to depend heavily on parameter values [8]. Second, without actual sensory input and motor output, it is difficult to tune these values to perform a specific function. Once this system is integrated with sensors and a mobile platform, parameters will be tuned more carefully to correspond to the rest of the system.

2.2   Example Process Flow Between PB and EB

The PB and EB work together to use sensory information from head sensors to update the animal's internal representation of its orientation. Incoming motion cues, assumed to already be side-biased prior to reaching the central complex, feed into the preferred side of the protocerebral bridge. When the body starts to rotate, sensory organs sensitive to rotation generate neural activity proportional to rotational speed. This neural activity evenly disinhibits all eight columns of one half of the protocerebral bridge, while the other half remains inhibited due to a lack of sensory input.

Figure 2 illustrates a concrete example to illustrate the process flow of the CX for signal integration and is used to give an idea of the sequence of events that must take place for the activity bumps to move in our model. In this example, the animal is originally at rest, and thus, no input signal is yet being received. However, a memory trace is maintained from the last known body position of $0°$, which corresponds to wedge one being active (Fig. 2A). This memory trace continuously sends a signal bilaterally through the E-PG axons to PB column one cells, but this signal from EB wedge one will not elicit depolarization. This is because at this point, the PB columns are being suppressed by the interneurons. The interneurons will continue to suppress the PB until body motion recommences, at which point the resulting sensory input inhibits the interneurons. It is the combination of receiving a signal from EB wedge one and the sensory input (Fig. 2B) causing disinhibition of the right protocerebral bridge that permits the first column of the right PB to activate (Fig. 2C); the activated first column of the right PB sends a signal via the P-EN axon, which articulates with the counterclockwise wedge eight of the EB, and now the activity bump of the EB has moved from wedge one to wedge eight (Fig. 2D). If the body continues to rotate, the wedge activity is again transmitted, bilaterally, to columns eight of the left and right PB, and the activity bump in the PB now moves from columns one to columns eight on both sides. This sequence of events will continue as long as body motion is present.
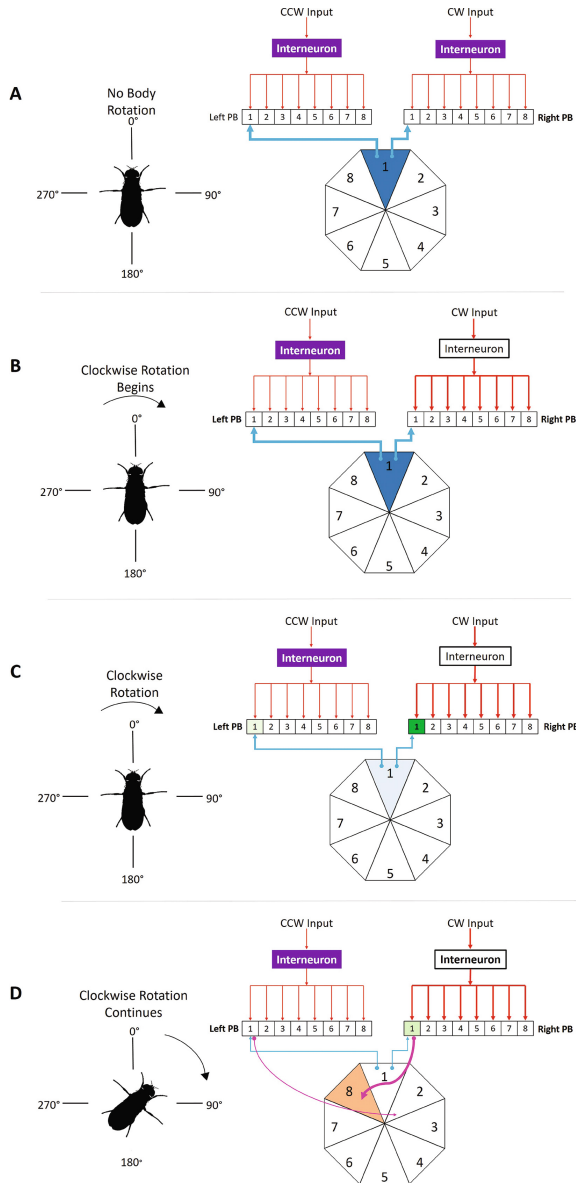
Fig. 2. Demonstration of the step-wise process flow of signal transduction within the CX. (A) The body is at rest at a reference point of 0°. The corresponding wedge has sustained voltage activity due to a memory trace of this known position - even while at rest. (B) CW body motion starts which causes a proportional current to feed into the preferred side of the PB, indicated by thicker red input lines. (C) The memory trace activity is passed symmetrically via the E-PG to the first columns of the PB. Because only the right side is disinhibited by sensory feedback, only the right first column of the PB depolarizes, as indicated by the dark green of column one. (D) As the body motion continues, the right PB remains disinhibited, thereby allowing the right PB column one to pass the activity in a counterclockwise fashion to wedge eight. (Color figure online)

2.3   Model Behavior

With the model assembled, we tested if our *in silico* CX behaves similarly to the *in vivo* CX. Several key behaviors were seen empirically that we wanted to ensure our model can reproduce:
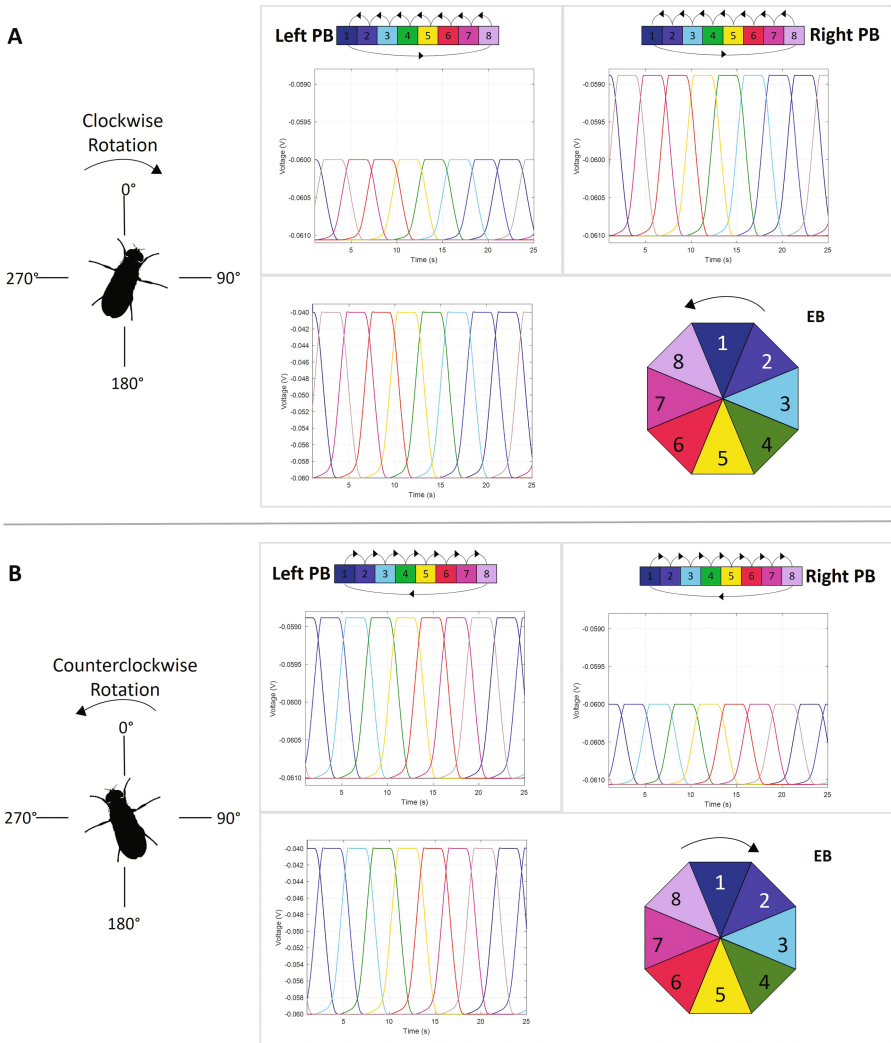
1. The direction of body rotation dictates direction of activity bump movement in the EB layer.
2. The body's rotational speed correlates to bump activity speed in the EB.
3. The activity in the PB leads activity in the EB.

Experimental studies show that when a fruit fly experiences clockwise motion in the yaw plane, the EB activity bump moves counterclockwise (Fig. 3A); the opposite is true for counterclockwise body motion (Fig. 3B). The connectivity is such that when the preferred side of the PB is disinhibited (and the non preferred side remains inhibited) the signal is able to move up the column (EB to PB) and is passed by the PB back to the EB in a counterclockwise fashion, thus causing counterclockwise bump movement.

When the body rotates at a faster speed, the incoming current from sensory organs to the CX is presumably greater in magnitude. This permits disinhibition of the preferred side PB to a greater degree and as a result, enables the EB to depolarize the PB more quickly. Figure 4A shows the activity of one EB wedge over time, for three different values of incoming sensory current. It is clear that the frequency of bursts increases with increasing sensory current. Figure 4B plots the summary of these, and additional trials, showing that the disinhibitory input to the PB monotonically controls the speed of bump motion in the EB.

The profile of activation and deactivation in the PB and EB also depend on the incoming current from sensory organs to the CX. Figure 4C shows the activity in the left protocerebral bridge (LPB), right protocerebral bridge (RPB), and ellipsoid body (EB) given different input currents. Figure 4C shows that the RPB is disinhibited due to it being the preferred side in this scenario, and that the voltage profile is highly dependent on input speed. In slow rotation (1nA input - corresponding to a 5% max body speed), the PB neurons slightly depolarize above resting potential and take a relatively longer time to do so as indicated by the less steep voltage trace. Faster speeds (10nA and 20nA inputs - corresponding to a 50% and 100% max body speed, respectively) allow for a greater degree of disinhibition, resulting in high depolarization magnitudes and faster rise times. Ultimately, stronger depolarization of the PB results in faster bump hand-off in the EB.

The EB bump profiles of Fig. 4C (bottom) show that these cells will depolarize to roughly the same degree, regardless of speed, but at different rates. Again, a slower rotational speed (i.e. weaker sensory input) results in slower depolarization. Although the synapses in our simulation saturate when the presynaptic voltage is greater than -40 mV, the voltage of the EB wedges may surpass this functional range.

Fig. 3. The direction of body rotation dictates the direction of bump activity movement. (A) CW body rotation results in left bump motion in the PB and CCW bump movement in the EB. (B) CCW body rotation results in left bump motion in the PB and CW bump movement in the EB. (Color figure online)

From our signal process flow example (Fig. 2) we hypothesized that an EB wedge (or combination of wedges) must have sustained activity that serves as a memory trace of the last known position after the body motion has stopped. This memory trace serves as a starting point for the activity bump when body motion recommences. Although the memory trace originates in the EB wedge, it is the disinhibition of the PB that permits the bump to start moving to neighboring
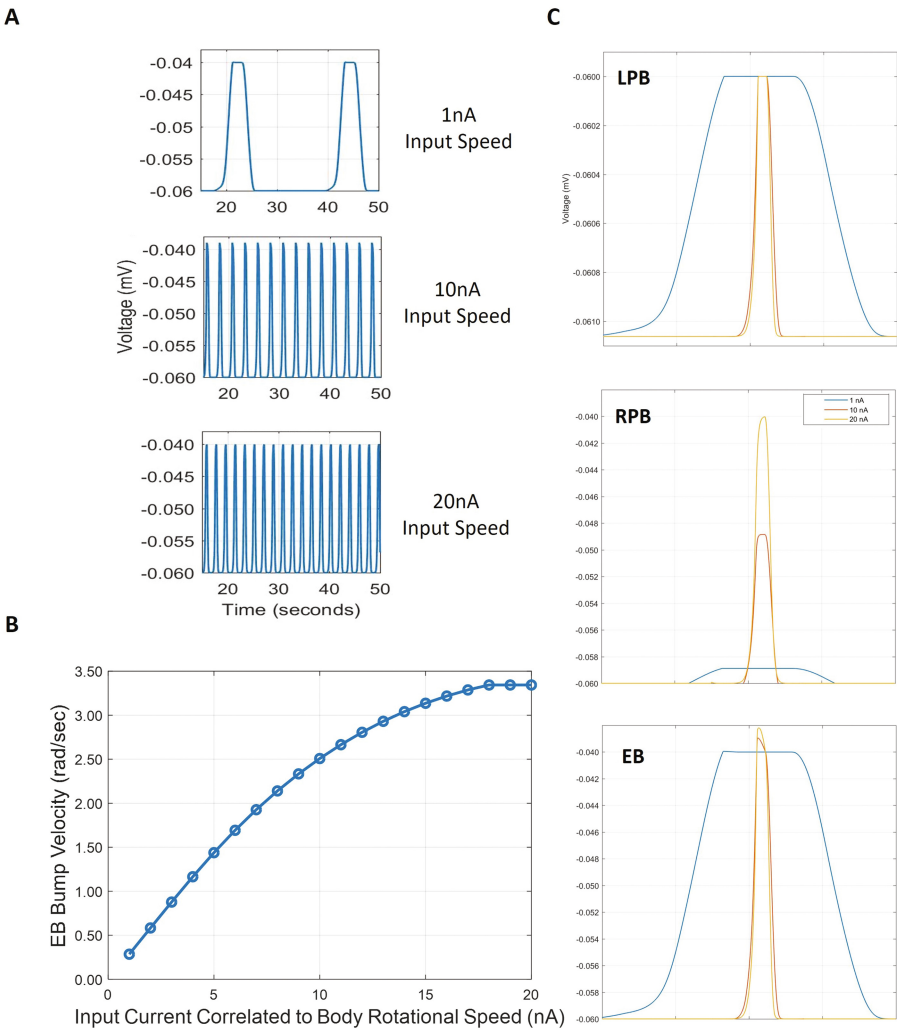
Fig. 4. Body rotational speed correlates with the bump speed in the PB and EB, while also correlating depolarization magnitude of the preferred side PB. (A) Fast body rotation (input as current with increasing magnitudes) causes faster bump hand-off in the EB (rad/sec). (B) Bump profiles in the left PB (top), right PB, preferred side (middle), and EB (bottom). Rotational speed effects the depolarization speed of the EB and PB cells, while greatly affecting the depolarization magnitude of the preferred side PB (right, in this case). (C) Example of period between bumps in the EB for slow (1nA), medium speed (10nA) and fast (20nA) rotational speeds. (Color figure online)

wedges. In a sense, the PB serves as a gatekeeper in allowing the bump to be passed and as such, its activity must precede that of the EB. This can be seen in the last step of Fig. 2D, where it is the activation of the PB that permits the EB to pass the bump.

3   Discussion

In this paper, we presented a model of the central complex that is able to mimic key neuronal behaviors seen in the brain of the fruit fly. Specifically,

1. The direction of body rotation dictates direction of activity bump movement in the EB layer.
2. The body's rotational speed correlates to bump activity speed in the EB.
3. The activity in the PB leads activity in the EB.

Utilizing the excitatory loop architecture between the PB and EB, we were able to produce a model that appropriately responded to body position and speed.

Tracking Body Position with Multimodal Sensory Inputs: Further work will incorporate how environmental stimulation is received by sensory organs and processed upstream to the central complex. More specifically, we wish to explore the interplay between sensory types and how they are prioritized within the central complex or how they may be modulated upstream to the CX. Varga and Ritzmann (2016) reported that units in the CX showed orientation-dependent activity both when a visual landmark was provided, and when it was removed [12]. This suggests that other organs, such as chordotonal organs (COs) in the antennae, sense the motion of the body and also stimulate the CX. In the future, we wish to explore the possible upstream interplay between visual inputs and CO inputs from the antennae. Specifically, how do different environmental conditions (i.e. the presence of visual cues) modulate the CO inputs? How does the total absence of visual input affect the gain of CO input, and thus the strength of these inputs during sensory integration found in the EB? Lastly, how does this inertial pathway (i.e. CO feedback) that feeds into the EB get used in position determination, spatial memory, and coordination of fine movement in downstream networks? Using extracellular CX recordings from cockroaches, we plan to explore how one sensory modality affects the strength of input to the CX, and correlate these sensory signals with CX activity.

Expanding Model to Include Other CX Neuropils and Brain Structures: Additionally, we wish to expand our CX model to include more processing layers of the EB, integrate the fan-shaped body (FB), and expand beyond the CX. One cell type we wish to include in future models are the ring cells of the EB. As the name implies, these cells are concentrically organized in four distinct rings at various depths of the EB [9,14,15], and neurophysiology work has shown that they participate in object tracking [15]. In brief, the innervation of these EB cells appears to come from a visual stimulation pathway that feeds through the

lateral triangles and into the appropriate EB ring network depending on object location within the visual field. It is our goal to construct a model that simulates the visual activation and the downstream neural dynamics of this pathway. We will then explore how this object tracking pathway, in conjunction to the inertial pathway described above, is used in spatial memory and movement coordination. The FB is thought to be the receiver of these various pathways and serves as the locus of coordination and decision making that may be the key to defining appropriate behavioral responses to experienced stimuli [5].

Tying It All Together: In summary, our results show that a simple neuronal architecture can effectively maintain real-time body position updates. This model, and the future work discussed here, serve as a first step in capturing the adaptive capabilities of the arthropod nervous system. With a better understanding of these situational neuronal behaviors seen in arthropods [6,7], our models can be used as a framework for robotic control where we hope to see improved adaptability.

References

1. Cofer, D., Cymbalyuk, G., Reid, J., Zhu, Y., Heitler, W.J., Edwards, D.H.: AnimatLab: a 3D graphics environment for neuromechanical simulations. J. Neurosci. Methods **187**, 280–288 (2010)
2. Fiore, V.G., Kottler, B., Gu, X., Hirth, F.: In silico interrogation of insect central complex suggests computational roles for the ellipsoid body in spatial navigation. Front. Behav. Neurosci. **11**(142), 1–13 (2017)
3. Green, J., Adachi, A., Shah, K.K., Hirokawa, J.D., Magani, P.S., Maimon, G.: A neural circuit architecture for angular integration in Drosophila. Nature **546**(7656), 101106 (2017)
4. Heinze, S.: Neural coding: bumps on the move. Curr. Biol. **27**(11), R409–R412 (2017)
5. Pfeiffer, K., Homberg, U.: Organization and functional roles of the central complex in the insect brain. Annu. Rev. Entomol. **59**, 165–184 (2014)
6. Ritzmann, R., Harley, C.M., Daltorio, K.A., Tietz, B.R., Pollack, A.J., Bender, J.A., Guo, P., Moromanski, A.L., Kathman, N.D., Nieuwoudt, C., Brown, A.E., Quinn, R.D.: Deciding which way to go: how do insects alter movements to negotiate barriers? Front. Neurosci. **6**, 97 (2012)
7. Varga, A.G., Kathman, N.D., Martin, J.P., Guo, P., Ritzmann, R.E.: Spatial navigation and the central complex: sensory acquisition, orientation, and motor control. Front. Neurosci. **11**, 4 (2017)
8. Stone, T., Webb, B., Adden, A., Weddig, N.B., Honkanen, A., Templin, R., Wcislo, W., Scimea, L., Warrant, E., Heinze, S.: An anatomically constrained model for path integration in the bee brain. Curr. Biol. **27**, 3069–3085
9. Su, T.S., Lee, W.J., Huang, Y.C., Wang, C.T., Lo, C.C.: Coupled symmetric and asymmetric circuits underlying spatial orientation in fruit flies. Nat. Commun. **8**(1), 139 (2017)
10. Szczecinski, N.S., Hunt, A.J., Quinn, R.D.: A functional subnetwork approach to designing synthetic nervous systems that control legged robot locomotion. Front. Neurorobot. **11**, 37 (2017)

11. Turner-Evans, D., et al.: Angular velocity integration in a fly heading circuit. Elife **6**, 139 (2017)
12. Varga, A.G., Ritzmann, R.E.: Cellular basis of head direction and contextual cues in the insect brain. Curr. Biol. **26**, 1816–1828 (2016)
13. Wolff, T., Iyer, N.A., Rubin, G.M.: Neuroarchitecture and neuroanatomy of the Drosophila central complex: a GAL4-based dissection of protocerebral bridge neurons and circuits. J. Comp. Neurol. **523**(7), 997–1037 (2015)
14. Young, J.M., Armstrong, J.D.: Structure of the adult central complex in Drosophila: organization of distinct neuronal subsets. J. Comp. Neurol. **518**(9), 1500–1524 (2010)
15. Seelig, J.D., Jayaraman, V.: Feature detection and orientation tuning in the Drosophila central complex. Nature **503**(7475), 262–266 (2013)